The Role of Bay of Bengal Convection in the Onset of the 1998 South China Sea Summer Monsoon

YIMIN LIU

State Key Laboratory of Numerical Modeling for Atmospheric Sciences and Geophysical Fluid Dynamics (LASG), Institute of Atmospheric Physics, Chinese Academy of Sciences, Beijing, and Laboratory for Atmospheric Research, Department of Physics and Materials Science, City University of Hong Kong, Hong Kong, China

JOHNNY C. L. CHAN

Laboratory for Atmospheric Research, Department of Physics and Materials Science, City University of Hong Kong, Hong Kong, China

JIANGYU MAO AND GUOXIONG WU

State Key Laboratory of Numerical Modeling for Atmospheric Sciences and Geophysical Fluid Dynamics (LASG), Institute of Atmospheric Physics, Chinese Academy of Sciences, Beijing, China

(Manuscript received 8 January 2002, in final form 1 May 2002)

ABSTRACT

Assimilated analysis fields from the South China Sea Monsoon Experiment and the outgoing longwave radiation data from the National Center for Atmospheric Research (NCAR) have been employed to describe the large-scale and synoptic features of the subtropical circulation during the Bay of Bengal (BOB; 6°–20°N, 80°–100°E) and South China Sea (SCS; 7°–20°N, 110°–120°E) monsoon onsets in 1998. The results show that the Asian monsoon onset during May 1998 exhibited a typical eastward development from the BOB region to the SCS domain. The weakening and retreat of the subtropical anticyclone from the SCS were preceded by the intrusion of westerlies and the development of convective activities over the northern part of the SCS (NSCS; 15°–20°N, 110°–120°E). As the vertical shear of zonal wind changes in sign, the ridge surface of the subtropical anticyclone tilted northward and the summer pattern was established over the SCS. Based on these observational results, version 4 of the NCAR climate model (CCM3) is used to investigate the physical link between the convection associated with the BOB monsoon vortex and the SCS summer monsoon onset, as well as the mechanism of the evolution of the low-level subtropical anticyclone over the SCS.

Introduction of heating over the BOB results in vigorous convection over the BOB, and the BOB monsoon onset, as well as the development of westerlies and vertical ascent over the NSCS region due to an asymmetric Rossby wave response. Together with the low-level moisture advection, convection is induced over the NSCS. It is the condensation heating over the NSCS that causes the overturning of the meridional gradient of temperature over the SCS. Consequently the subtropical anticyclone in the lower troposphere over the SCS weakened gradually. Eventually as convection develops over the entire SCS domain, the subtropical anticyclone moves out of the region.

1. Introduction

The Asian monsoon is one of the largest circulation systems on earth. Its seasonal transition from winter to summer in east and south Asia is characterized by abrupt changes in the general circulation. Tao and Chen (1987) suggested that the earliest onset of the Asian summer monsoon (ASM) occurs over the South China Sea (SCS). However, as more observations and reanalysis data became available in the 1990s, it was found that the ASM onset appears to have the following general sequence: first, over the Bay of Bengal (BOB; 6°–20°N, 80°–100°E), then the South China Sea, and lastly south Asia. Wu and Zhang (1998) demonstrated this for the 1989 case while Xu and Chan (2001) obtained a similar result for the 1998 onset. Lau et al. (1998) also observed a monsoon depression over the BOB in 1997, in the preonset stage of the SCS summer monsoon (SCSSM). Lau et al. (2000) found this to be repeated in 1998 and during the Joint Air–Sea Interaction Experiment in May 1999. During the period of 1975–98, Wu and Chan (2000) often observed the phenomenon of BOB convection preceding the SCS monsoon onset. Indeed, Zhang and Wu (1998), Fong and Wang (2001) and Mao

Corresponding author address: Dr. Yimin Liu, LASG, Institute of Atmospheric Physics, Chinese Academy of Sciences, P.O. Box 9804 Beijing 100029, China.
E-mail: lym@lasg.iap.ac.cn

et al. (2002) also reported such a three-stage feature in the ASM onset in the climate mean.

In 1998, the South China Sea Monsoon Experiment (SCSMEX) over the SCS studied the physical processes associated with the SCSSM (detailed descriptions of this experiment and observation methodologies can be found in Lau et al. 2000). Based on the data collected during the experiment, investigations have been performed to identify the structure and evolution of the circulations of the 1998 SCSSM, as well as the triggering mechanism of its onset (Lin et al. 1998; Ding and Li 1999; Ding and Liu 2001; Chan et al. 2000; Xu and Chan 2001). The general consensus is that during 1998, the earliest onset occurred over the northern SCS around 15–17 May. The SCS monsoon then developed over the entire SCS region around 20–25 May, which heralded a change in the large-scale monsoon circulation pattern. Chan et al. (2000) showed that the meridional circulation and high relative humidity were already established in early May over the SCS. A tropical cyclone over the Bay of Bengal apparently provided a conduit for the transport of moisture to the SCS. From 21 May onward, low-level westerlies prevailed over the central and southern SCS, in association with the ''eastward retreat'' of the subtropical anticyclone in the lower troposphere. These shifts in large-scale circulation signaled the full onset of the SCS monsoon (Lau et al. 2000). However, if the circulation is examined closely, the center of subtropical anticyclone at low levels did not vary much during the SCS monsoon onset. It was only the western extent of the subtropical anticyclone that ''disappeared.''

These observations related to the SCSSM onset in 1998, together with those from some of the more recent studies, highlight two important issues. First, it is apparent that a BOB cyclone, and the BOB summer monsoon onset, appeared before the SCSSM onset. Are these two onset events physically linked? Second, does the low-level subtropical anticyclone really ''retreat'' eastward, or is this retreat simply a manifestation of the weakening of its western portion over the SCS? In either case, what is the physical mechanism involved? Both issues form the basic objectives of the present study, which is carried out through numerical simulations.

The relation between these two issues may not be immediately apparent. However, recent studies (see discussion later) have related the formation and variation of the subtropical anticyclone to condensational heating, which should be an important physical process associated with the BOB cyclone and monsoon onset. Therefore, it is useful to review such a relationship to provide the necessary background for future discussions.

Since the ridge axis of the subtropical anticyclone in the Northern Hemisphere separates westerlies to the north and easterlies to the south, the isotach of zonal wind $u = 0$, where the meridional gradient of u is positive, can be used to represent this axis. A ridge surface can then be defined as one that intersects a pressure surface at the ridge axis of the subtropical anticyclone on that pressure surface. The ridge surface thus bounds the westerly to the north and easterly to the south. Thermal wind balance requires the ridge surface, which is roughly zonally oriented, to tilt towards the warmer region with height. In the Asian monsoon area, this region is to the south in winter but to the north in summer. Therefore the seasonal transition from winter to summer at a location is characterized by the appearance of a vertical ridge surface, which is accompanied by the monsoon onset and labeled by Mao et al. (2002) as the ''seasonal transition axis'' (STA). In the eastern portion of the ASM region, such a transition appears at the lower troposphere as the eastward retreat of the subtropical anticyclone.

In their studies of the lower-tropospheric subtropical circulations in both summer and winter, Hoskins (1996), Rodwell and Hoskins (1996), and especially Rodwell and Hoskins (2001), found that over the western North Pacific, the easterlies associated with the subtropical anticyclone in the summer are primarily a ''response'' to Asian monsoon heating, while in winter, the interaction between the zonally averaged flow and the mountains gives the zonally asymmetric subtropical circulation. However, their work did not consider the evolution of the subtropical anticyclone during the seasonal transition period. Furthermore, the diabatic heating used in these studies was obtained from analysis data as a residual of the thermodynamic equation. This makes it difficult to distinguish the contributions of latent heating to the formation of the subtropical anticyclone versus other kinds of diabatic heating. Chen et al. (2001) also investigated the origin of the Northern Hemisphere subtropical anticyclone using a linear quasigeostrophic model, but focused only on the summer season as well.

Recent studies by Wu and his collaborators (Wu et al. 1999; Liu et al. 2001a) have shown that different kinds of external forcing as well as internal forcing have different impacts on the formation and variation of the subtropical anticyclone from the vorticity perspective. Wu et al. (1999) derived a complete vorticity equation (CVE) that is exactly equivalent to the Ertel potential vorticity equation (Ertel 1942). The CVE includes explicit dynamical and thermodynamic elements, such as frictional dissipation and diabatic heating. When only diabatic heating is included, a scaling analysis of the quasi-steady response of the circulation along the subtropical ridge axis gives the following result:

$$\beta v \propto \frac{f + \zeta}{\theta_z}\frac{\partial Q}{\partial z}, \qquad \theta_z \neq 0, \tag{1}$$

where $\theta_z = \partial\theta/\partial z$, ζ is the vertical component of relative vorticity, v the meridional wind, β the variation of the Coriolis parameter f with latitude, θ the potential temperature, and Q the diabatic heating. The deep convective condensation heating will form an isolated subtropical anticyclone in the lower troposphere to the east

of the heating (Wu et al. 1999; Liu et al. 2001a; Rodwell and Hoskins 2001). The southerly to the west of such an induced subtropical anticyclone, if it is over the ocean, will bring plenty of moisture to the west and northwest of the subtropical anticyclone, contributing to the development of convection and condensation heating over there. If this occurs just before the monsoon onset and the condensation heating to the north of the subtropical anticyclone has accumulated to a certain extent, the wintertime (negative) meridional temperature gradient across the ridge axis will change sign, and the tilting of the ridge axis will change from the winter to the summer pattern. Monsoon onset will then be triggered and the subtropical anticyclone will appear to have retreated eastward.

The objective of this work is to verify the previous hypothesis that the condensation heating over the northern SCS acts to reverse the winter horizontal temperature gradient over the SCS, and to study the impacts of condensation heating associated with the BOB monsoon onset on the circulation over the SCS prior to the SCS summer monsoon onset using numerical experiments. Although some analyses have been carried out on the synoptic-scale features associated with the 1998 SCSSM onset (see references in the beginning of this section), it is useful to describe briefly the evolution to provide the background for evaluating the model results. Such an overview of the SCSSM onset is first given in section 2. The data used are the SCSMEX dataset provided by the Beijing Data Center of SCSMEX for the period of 1 to 30 May 1998, and the interpolated outgoing longwave radiation (OLR) obtained from the National Center for Atmospheric Research (NCAR). The former contains 6-hourly assimilated regional analyses at 11 levels (1000, 925, 850, 700, 500, 400, 300, 250, 200, 150, and 100 hPa) with a horizontal resolution of 1° latitude square in the region of 10°S–40°N 70°–150°E. The latter is the daily average with a horizontal resolution of 2.5° latitude square over the entire globe.

Although the focus here is on regional climate, the evolutions of local systems are studied in relation to the large-scale circulation. Therefore, a global model, the fourth version of the NCAR Community Climate Model (CCM3), is employed to simulate the BOB and SCS monsoon onsets and to investigate the influence of diabatic heating over the BOB on the monsoon onset over the SCS through sensitivity experiments. The model simulations are presented in section 3. It includes diagnoses of several idealized numerical experiments, and is followed by a conclusion and discussion in section 4.

2. Observational overview of the SCSSM onset

a. Daily features of the circulation over the SCS

To remove diurnal variations, a three-point temporal running mean is applied to the data at each grid point. The evolution of the 850-hPa zonal winds shows a band

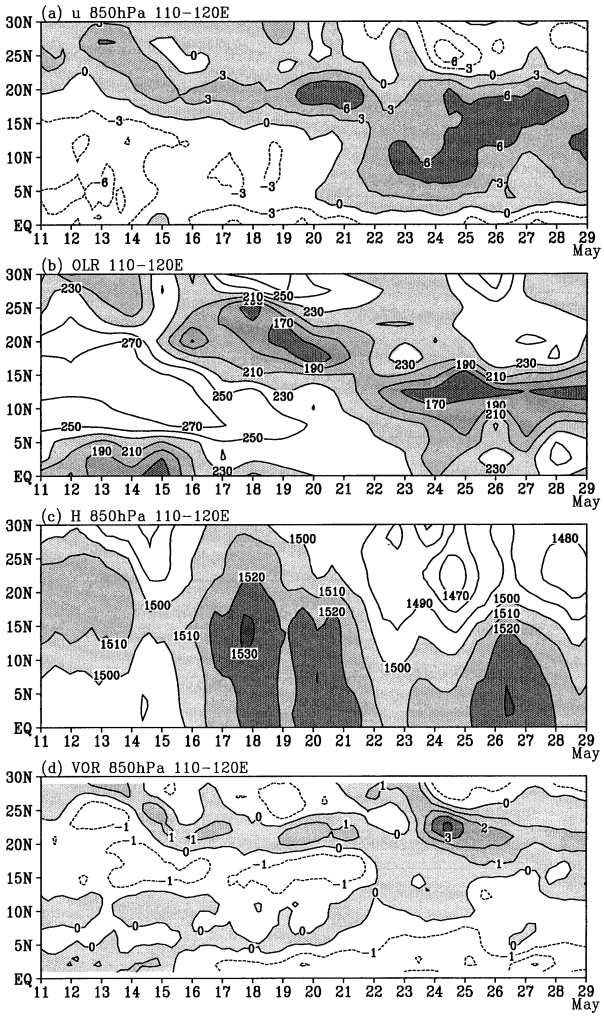

FIG. 1. Time–latitude cross section averaged within 110°–120°E from 11 to 29 May 1998 of (a) 850-hPa zonal wind u (m s^{-1}), shading for $u > 0$; (b) OLR (W m^{-2}), shading for OLR < 230 W m^{-2}; (c) 850-hPa geopotential height H (gpm), shading for $H > 1500$ gpm; and (d) 850-hPa relative vorticity ζ (10^{-5} s^{-1}), shading for $\zeta > 0$.

of westerlies over the northern part of the SCS before 20 May (Fig. 1a). Its intensity increases by 20 May and then jumps southward to dominate the entire SCS domain. The evolution of OLR (Fig. 1b) shows that no significant convection occurred over most of the SCS region until 16 May when strong convection developed in the northern SCS (NSCS). On 19 May convection intensified greatly over the NSCS and began to spread southward quickly. At the same time, the geopotential height at 850 hPa over the SCS region decreased rapidly from over 1520 gpm to ~1500 gpm (Fig. 1c), and the 850-hPa relative vorticity over the SCS became positive by 22 May (Fig. 1d).

These results are generally consistent with those of previous researchers (e.g., Li and Qu 1999; Chan et al. 2000) and suggest that the weakening of the subtropical anticyclone over the SCS was accompanied by the in-

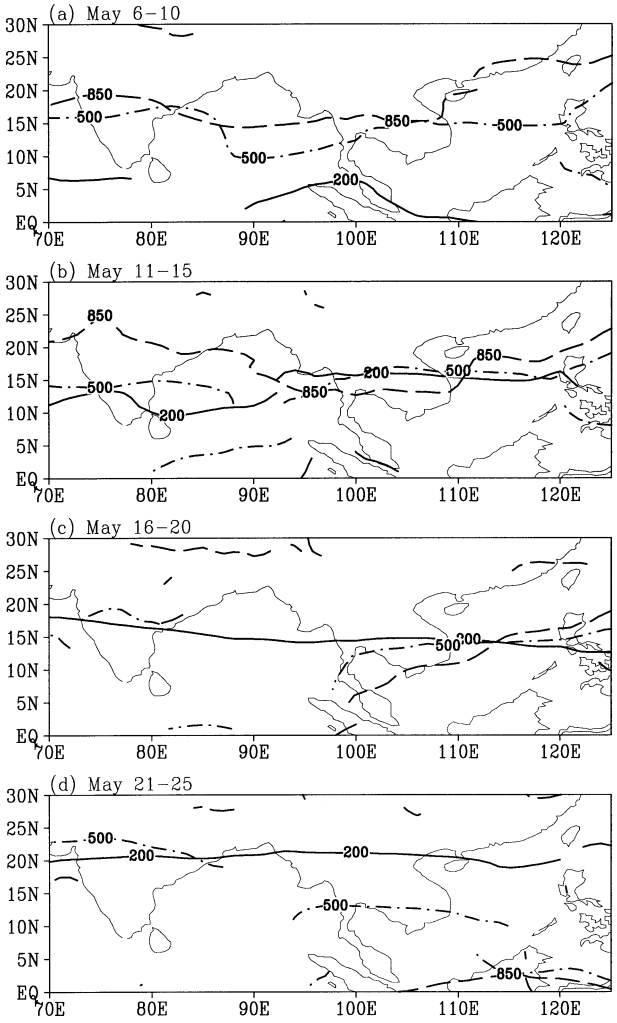

FIG. 2. The ridge axis (zero isotach of zonal wind *u* and meridional gradient of *u* positive) at 200, 500, and 850 hPa during the (a) second (6–10 May), (b) third (11–15 May), (c) fourth (16–20 May), and (d) fifth (21–25 May) pentads in 1998.

trusion of westerlies and the development of convective activities over the region, particularly over the NSCS.

b. Evolution of the subtropical anticyclone

Before the ASM onset, the subtropical anticyclone dominated the region from the BOB and SCS to the eastern Pacific at the lower troposphere (Fig. 2a). At this time (second pentad of May), the ridge of subtropical anticyclone at 200 hPa is to the south of that at 500 and 850 hPa, which shows a typical winter pattern, and the ridge line was continuous in the subtropical area. In the third pentad of May (Fig. 2b), the vertical shear of zonal wind has started overturning over the eastern part of the BOB, with the ridge surface almost vertical between 850 and 500 hPa along 15°N and appearing to tilt slightly northward with height from 500 to 200 hPa. Over Indochina, the 200- and 500-hPa ridge axes intersect. This indicated that during this pentad, the upper-tropospheric meridional temperature gradient over the eastern BOB and western Indochina has changed from the winter to the summer type.

The STA then migrated eastward and reached the SCS region during the fourth pentad, when the BOB monsoon onset had occurred and the ridge axis at 500 and 850 hPa broke up over the BOB (Fig. 2c). This indicates that over the BOB region, a trough had replaced the wintertime subtropical anticyclone in the midtroposphere. In the fifth pentad, the 850-hPa ridge axis over the SCS moved southward to the equatorial region (Fig. 2d), which suggests that westerlies prevailed over the entire SCS. The ridge surface tilted northward and the summer pattern had been established over the SCS.

c. Regional circulation characteristics over BOB and SCS

The results in the previous section clearly indicate that the seasonal transition from winter to summer in 1998 occurred in the third (fifth) pentad of May over the BOB (SCS). To establish a possible linkage between these two transitions, the circulation evolution between these two pentads is further examined here.

Previous studies (Chan et al. 2000; Lau et al. 2000) have pointed out an important feature associated with the onset of the 1998 SCS monsoon—an onset vortex over the northern Indian Ocean. Such a vortex generally develops into a tropical storm with an increase in the area of organized cloud cover (Krishnamurti et al. 1981). It is also interesting to note that the vortex revealed from satellite imagery was almost a repeat of the corresponding daily satellite observations during 1997 (Lau et al. 1998). On 13 May enhanced convective activity occurred over the southern part of the BOB with the center near (5°N, 90°E; Fig. 3a). It was accompanied by a vortex to the west and an anticyclone to the north and east. A band of convection also extended from Thailand to southern China. Although anticyclonic circulation dominated the northeastern part of the BOB and SCS at 850 hPa, the 200-hPa ridge axis was already to the north of that at 500 and 850 hPa over the eastern BOB (EBOB; Fig. 3b), which suggests that the seasonal transition over the BOB should occur soon.

Two days later (15 May), the circulation associated with the monsoon vortex strengthened (Fig. 3c), and the ridge axis at both 850 and 500 hPa have broken over the EBOB (Fig. 3d), which therefore implies the BOB monsoon onset. At this time, westerlies extended from the southeast of this vortex through the Indochina peninsula to the NSCS. On 17 May the monsoon depression intensified further and moved northward to 15°N (Fig. 3e). Over Thailand, the southwesterly flow met with the southeasterlies from the subtropical high over the SCS, leading to deep convection there. Although the tilt of the ridge surface over the SCS is still the winter pattern (Fig. 3f), it has decreased from the days before.

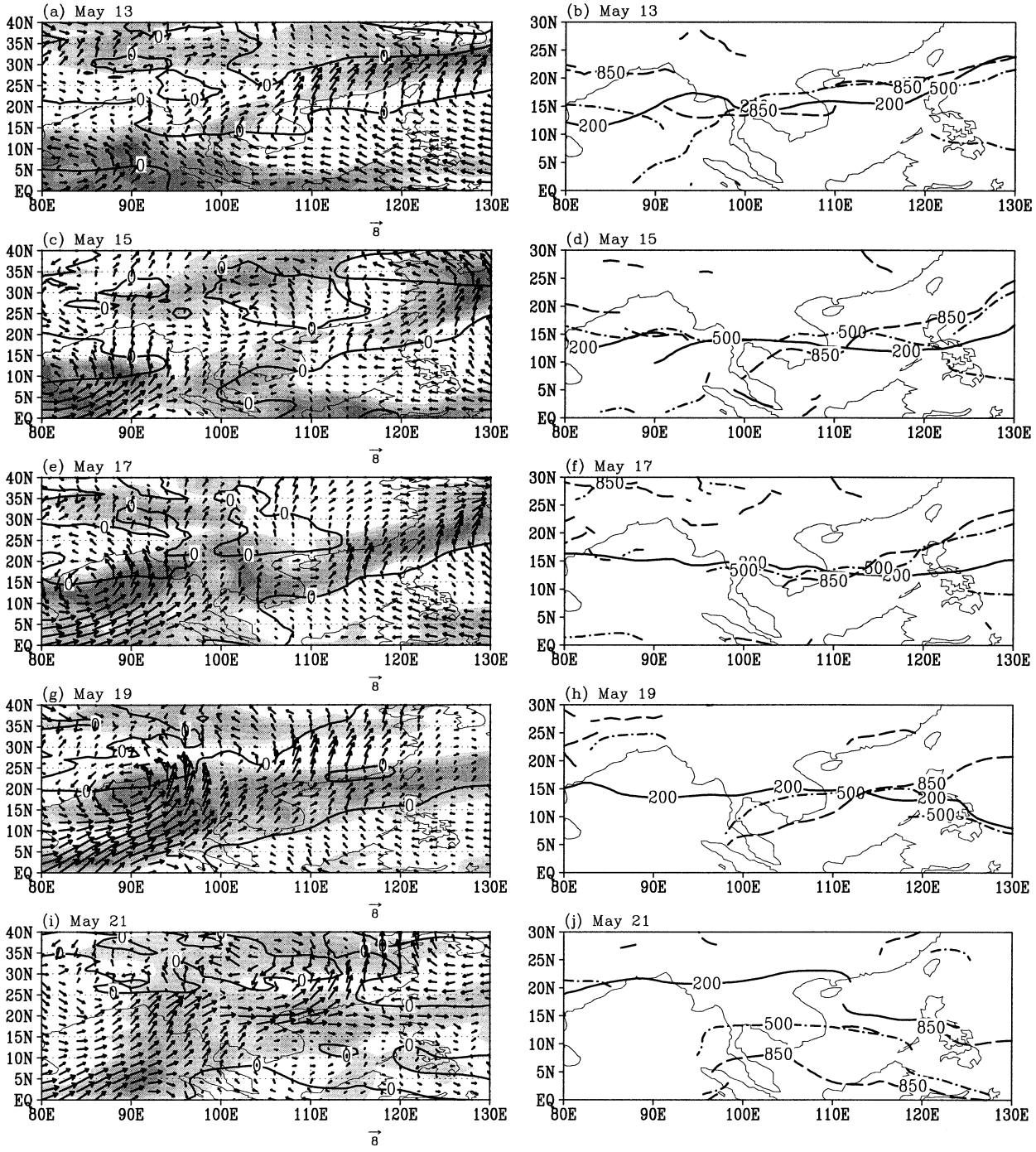

FIG. 3. Distributions of the daily 850-hPa wind vector (m s^{-1}, with zero isotach of zonal wind also plotted) and (left) OLR (shaded areas with OLR $<$ 230 W m^{-2}; interval: 20 W m^{-2}); and (right) subtropical ridge axis at 200, 500, and 850 hPa. Dates are labeled on each panel.

On 19 May convection over the NSCS became more active (Fig. 3g), and the STA is found over the central SCS (Fig. 3h), which means that the meridional gradient of temperature has turned from negative to zero, and heralds the beginning of the seasonal transition over this area. Two days later (21 May), the ridge axis at 850 hPa moved southward to the equatorial region over the SCS (Fig. 3j). Cyclonic flow prevailed over the NSCS and westerlies are found over the southern SCS (Fig. 3i, see also Fig. 1). The tilt of the ridge surface indicates that the summer pattern has been established over the whole SCS domain (Fig. 3j).

The change of the tilt of the ridge surface suggests that the meridional temperature gradient must also

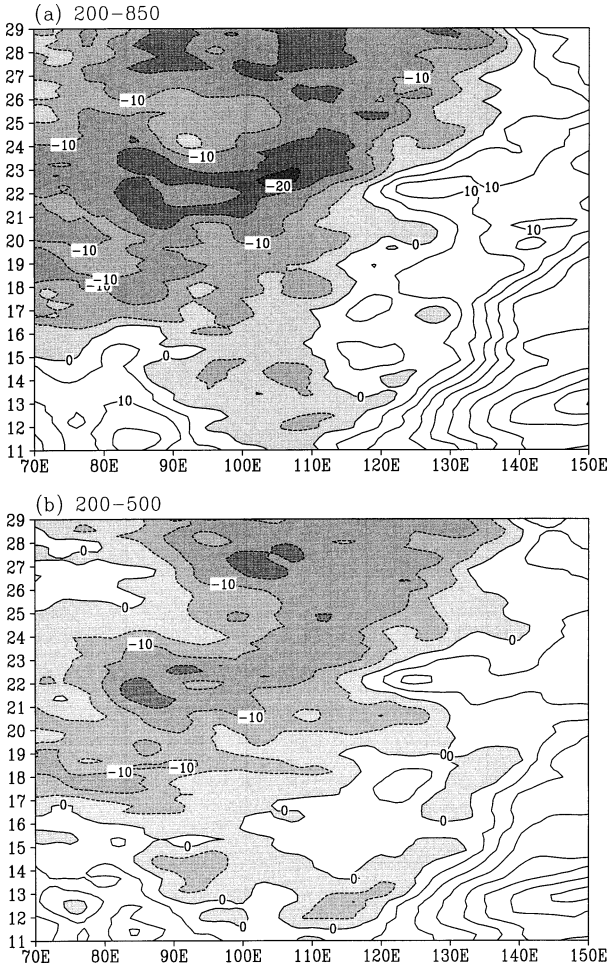

FIG. 4. Time–longitude cross section from 11 to 29 May (*y* axis) of the vertical shear of the zonal wind averaged within 11°–16°N between (a) 200 and 850 hPa, and (b) 200 and 500 hPa. Contour interval: 5 m s^{-1}.

change. Rather than examining such a gradient, the vertical shear of the zonal wind is analyzed. The zonal component of the thermal wind between both the 200–500- and the 200–850-hPa layers show that within either the entire troposphere (Fig. 4a) or the upper troposphere (Fig. 4b), the thermal wind changes from positive to negative first over the EBOB and Indochina peninsula region. However, a close comparison between Figs. 4a and 4b shows that the negative (easterly) vertical shear of zonal wind appears earlier in the midhigh troposphere (from 19 May) than in the whole layer (after 20 May) over the SCS. This indicates that the reversal of the meridional gradient of temperature in this region occurred first in the midhigh troposphere, which was likely caused by deep convective condensation heating over the NSCS. This is consistent with the OLR distributions (see Figs. 3e,g) in which the deep convection developed over the NSCS before the SCS monsoon onset. Furthermore, such development of deep convection followed the strengthening and northward movement of the BOB monsoon depression. This result suggests that in addition to the convection associated with the monsoon vortex over the BOB, which may enhance the westerlies over the SCS, the condensation heating over the NSCS may also be an important contributor. Chan et al. (2000) indicated that a cyclone from the midlatitudes might also play a role in the maintenance of the westerlies over the NSCS. The two processes might then work together to cause a weakening of the subtropical anticyclone over the SCS. Such reasoning will be tested using the CCM3 in the next section.

3. Model simulations

a. Brief model description

The NCAR CCM3 is a global spectral climate model. Its standard configuration includes a T42 horizontal spectral resolution (approximately a 2.8° lon × 2.8° lat transformed grid), 18 vertical levels, a top of 2.917 hPa, and a time step of 20 min. A complete description of the physical and numerical methods used in CCM3 can be found in Kiehl et al. (1996). Penetrative and shallow convection are parameterized using the Zhang and McFarlane (1995) and Hack (1994) schemes, respectively. With specified present-day sea surface temperatures (SST), CCM3 produces a globally and annually averaged balance between incoming solar radiation and OLR to <0.5 W m^{-2} (Boville and Gent 1998). In general, CCM3 is able to reproduce reasonably well the current observed climate, especially for the large-scale features and their seasonal cycle.

The model is initialized with the atmosphere and land data of 1 December provided by NCAR. An Atmospheric Models Intercomparison Project (AMIP) type-run is made with the forcing of the monthly SST with the annual cycle from December 1980 to March 1998. Started from 31 March 1998 in this AMIP II run, a control simulation (control run) of the evolution of the 1998 ASM is made by using specified weekly SST in 1998 (Reynolds and Smith 1994). The ability of the model to simulate the ASM onset will be described first in the next section, then followed by three sensitivity numerical experiments. Depending on which experiment, the model is initiated with either a zonal-mean field of 11 May of the control run or a ''real'' field of 12 May of the control run (see further description in the various experiments).

b. Control run

The simulated variations of the OLR over the SCS show that the model can generally model the three stages of the ASM onset, when compared with the observed OLR (Fig. 5). The simulated SCSSM onset characterized by the 190–210 W m^{-2} isoline is around 21–22 May, which is almost the same as that from observations. However, the simulated onset date for the onset

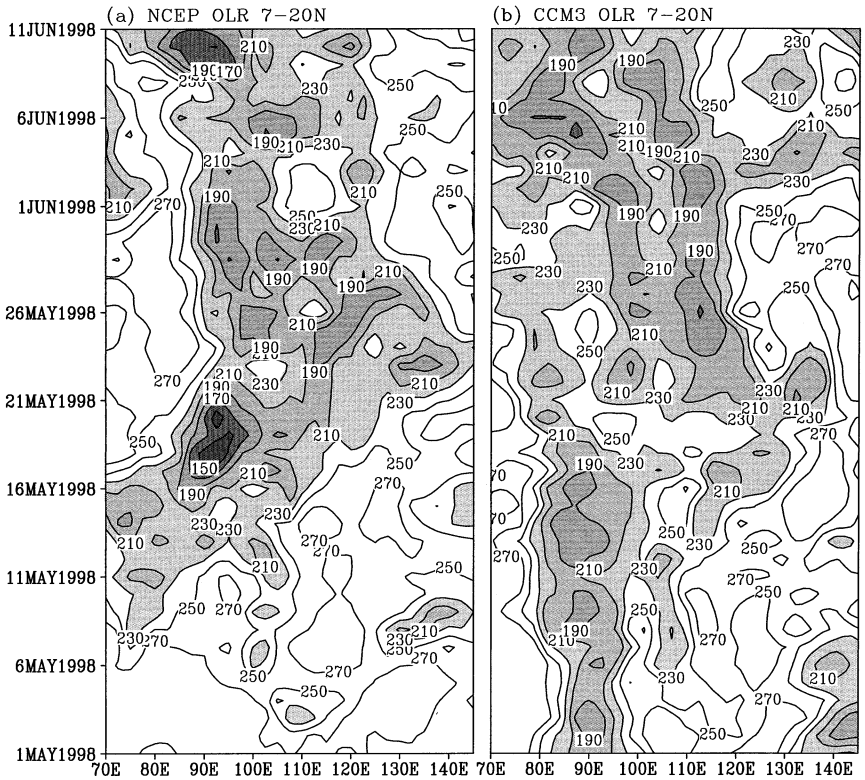

FIG. 5. Longitude–time cross section of OLR between 7°–20°N for the period 1 May to 11 June 1998 from (a) NCAR and (b) CCM3 simulations. Interval: 20 W m^{-2}. Shaded areas indicate values $<$230 W m^{-2}.

of the BOB monsoon is too early, and that for the Indian monsoon is also about 10 days earlier than that based on the observed OLR. In addition, the modeled OLR over the BOB and the Indochina peninsula during the BOB monsoon onset is higher than the observed values. The former reflects the model's ability to simulate the monsoon onset. The reason for the latter is that in the simulation before the SCSSM onset, to the south of 15°N, the averaged OLR during 15–20 May is larger than 230 W m^{-2} (Fig. 6a). Convection only develops in the northern part of Indochina during this period. The simulated convection over the southern part (100°–110°E) is too weak. But in the observation, convection developed strongly in the whole peninsula especially during 17–21 May (Figs. 3e,g,i).

The simulated circulation patterns also show distinct differences before and after 21 May (Fig. 6). Before 21 May there exists a very strong cyclone and vigorous convection over the BOB region (Fig. 6a). The low-level subtropical anticyclone dominates the vast area from Indochina through the SCS to the western Pacific. Westerlies, weak but with strong convection, are found over the NSCS. When compared with the observational results in Figs. 3e and 3g, the model can basically simulate the cyclonic circulation over the BOB and westerlies over the NSCS during the BOB monsoon onset. During 22–27 May westerlies prevail over the most areas of the SCS except its southeastern part, with strong convection throughout most of the SCS (Fig. 6b). The western edge of the subtropical anticyclone has moved from 95°E (Fig. 6a) to 112°E (Fig. 6b), but not as east as in the SCSMEX analysis (21 May, see Fig. 3i).

These diagnoses illustrate that although some discrepancies exist when compared with the reanalysis data, the CCM3 simulation results of the ASM onset should, in general, be acceptable. Thus, this model will be used to carry out sensitivity experiments to understand the physical processes involved in the changes in the large-scale features during the 1998 ASM onset.

c. Idealized condensation heating experiments

In the real world, the atmospheric response to condensation heating can be complicated by factors such as orography and sensible heating. Therefore, a better understanding of the problem can only be sought through idealized experiments. In the following experiments, no orography is used and an aqua-planet is assumed. The global surface sensible heating, which will be diffused into the free atmosphere, and radiation heat-

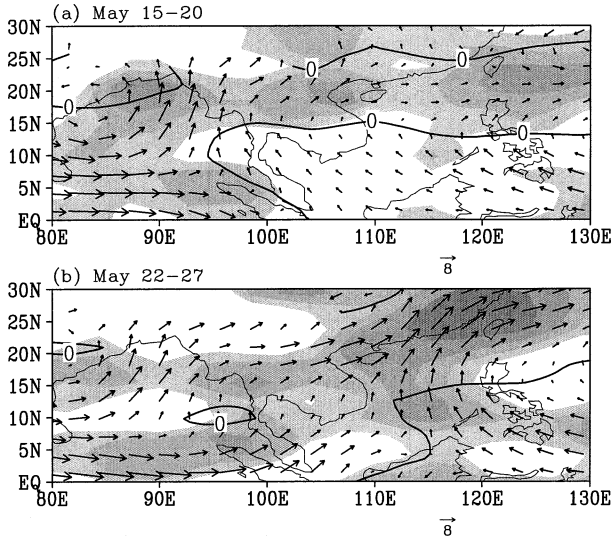

FIG. 6. Simulated (control run) 850-hPa wind vectors and OLR [only values of <230 W m^{-2} (shaded) shown, interval: 20 W m^{-2}] for a 6-day average between (a) 15–20 May (i.e., before the SCSSM onset) and (b) 22–27 May (after the onset). The heavy curve is the zero isotach of zonal wind at 850 hPa.

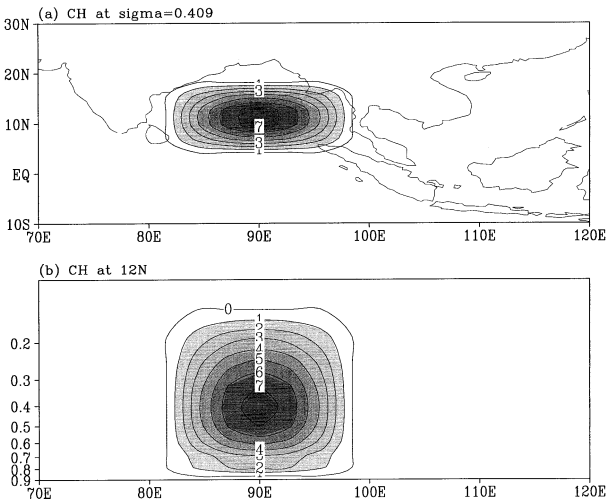

FIG. 7. Diabatic heating centered at 12°N, 90°E. (a) Plan view at $\sigma = 0.409$; (b) heating profile along 12°N. Contour interval: 1 K day^{-1}.

ing are turned off in the thermodynamic equation. Instead, an idealized ''monsoon'' heating source, which mimics the three-dimensional condensation heating distribution over the BOB during the onset period, is introduced into the model.

Results of two different idealized experiments will be presented in this section. One is without condensation heating generated by the model adjustment, and the other is with such heating. The former is to determine the effects of the prescribed latent heat release over the BOB alone. The latter means that when the model atmosphere is saturated, an induced latent heating is released due to the condensation process, the purpose of which is to examine the interaction between this heating and the large-scale flow.

Since the focus here is on the effect of the BOB monsoon onset vortex, a simple idealized elliptical heating centered at 12°N, 90°E is inserted over the BOB (Fig. 7). This idealized heating is representative of deep convection with a maximum of 8 K day^{-1} at ~400 hPa (Liu et al. 2001a; Rodwell and Hoskins 2001). The model is initiated with the zonal means of the 11 May circulation derived from the control simulation in the last section.

1) HEATING WITHOUT LARGE-SCALE ADJUSTMENT (CH1 RUN)

In this experiment (CH1 run), the large-scale is not allowed to have any latent heat release. The BOB heating is turned on at day zero. At day 1, a cyclone with positive vorticity is forced in the lower troposphere above the heating area (Fig. 8a), whereas in the upper troposphere an anticyclone with negative vorticity can be identified (not shown). This is because during a very short period of time, similar to Eq. (1), we know that

$$\frac{\partial \zeta}{\partial t} \propto \frac{f + \zeta}{\theta_z} \frac{\partial Q}{\partial z}, \qquad \theta_z \neq 0. \tag{2}$$

Therefore, in the lower troposphere where heating increases with height, positive cyclonic vorticity is generated, while in the upper atmosphere, the opposite is obtained.

The vorticity center enhances strongly with time (Figs. 8b,c). Besides this local effect, the heating generates a westward-moving Rossby wave. As in the case reported by Liu et al. (2001a), this feature agrees qualitatively well with the analytical results of Gill (1980).

For a steady state and below the maximum heating level $H_{\max}$ (at about 400 hPa) Eq. (1) becomes

$$\beta v \propto \frac{f + \zeta}{\theta_z} \frac{\partial Q}{\partial z} > 0, \qquad \theta_z \neq 0, \qquad z < H_{\max}. \tag{3}$$

Southerlies are therefore forced. A low-level subtropical cyclone center then appears on the western side of the deep condensation heating; whereas an anticyclone center appears on the eastern side of the deep condensation heating. Such a pattern can be found from day 5 (Fig. 5b). Southerlies prevail over the heating region, and cyclonic and anticyclonic flows are formed, respectively, to the west and east of the heating region. Thus the prescribed zonally symmetric anticyclone belt is disturbed by the diabatic heating, with the resultant pattern depending upon the vertical profile of the heating [Eq. (3)], as discussed by Wu et al. (1999).

In addition, an anticyclone appears just to the northern rim of the heating region from day 5 (Fig. 8b). This is because a negative vorticity forcing is generated to the north of the heating region by horizontal inhomogeneous

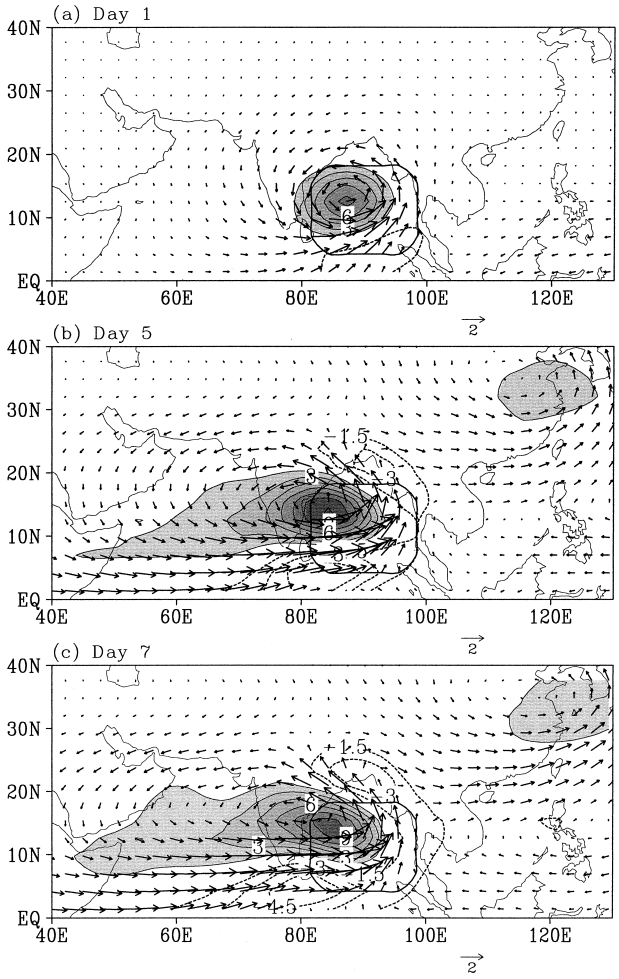

FIG. 8. Relative vorticity (10^{-6} s^{-1}; positive: shaded; negative: dashed) and horizontal wind vector (m s^{-1}) at 850 hPa generated from the CH1 run on (a) day 1, (b) day 5, and (c) day 7. Both parameters are deviations from the zonal mean. The heavy curve indicates heating region of >0.5 K d^{-1} at $\sigma = 0.409$.

heating. In fact, applying the thermal wind relation, the forcing of horizontal inhomogeneous heating in the CVE equation can be written as (Wu et al. 1999):

$$\left(\frac{\partial \zeta}{\partial t}\right)_x \propto -\frac{1}{\theta_z}\frac{\partial v}{\partial z}\frac{\partial Q}{\partial x} = -\frac{g}{fT\theta_z}\frac{\partial T}{\partial x}\frac{\partial Q}{\partial x}$$

$$\left(\frac{\partial \zeta}{\partial t}\right)_y \propto \frac{1}{\theta_z}\frac{\partial u}{\partial z}\frac{\partial Q}{\partial y} = -\frac{g}{fT\theta_z}\frac{\partial T}{\partial y}\frac{\partial Q}{\partial y}, \qquad (4)$$

where $\theta_z \neq 0$. Therefore, within the heating region as well as in the surroundings, as the air column over the heating region is warmed up, the horizontal gradient of temperature is in phase with that of the diabatic heating and negative vorticity is produced. In the lower troposphere, the southerly flow within the heating region is subjected to such negative vorticity forcing and turns clockwise (Liu et al. 2001a,b). Such induced anticyclonic westerlies prevail over southern China and extend into the northern part of the SCS (Figs. 8b,c). These westerly winds are important to the SCSSM onset (Chan et al. 2000).

2) HEATING WITH LARGE-SCALE ADJUSTMENT (CH2 RUN)

In this experiment (CH2 run), the large-scale condensation heating is switched on along with the imposed BOB heating. At day 1, the circulation responses are almost the same as those in CH1 (cf. Figs. 8a and 9a). However, the heating intensified quickly due to the switched-on large-scale condensation processes. As a result, the forced local cyclone over the BOB is much stronger by day 3 (Fig. 9c). From day 5, the forced circulation pattern over the SCS and western Pacific is similar to that in CH1 run (cf. Figs. 8c and 9c), and the model-induced condensation heating starts to spread northeastward through the westerlies associated with the Rossby wave train. The formation of such northeastward heating is also due to the ascent as well as moisture advection in the lower troposphere (Fig. 10). The ascent motion dominates the SCS region, especially in its northern part (Fig. 10a). This can be considered as the Rossby wave response to the BOB heating (Gill 1980). A close examination of the vertical heating distribution shows that the model-induced heating is concentrated in the mid and upper troposphere, similar to that in the prescribed heating. The combination effects of the prescribed heating and the induced heating make the southerly winds over the Indochina peninsula stronger than those in Fig. 8. However, the westerlies over the Indochina peninsula and the SCS region in both experiments are almost the same on days 5 and 7. This is because these westerlies are a part of the Rossby wave response to the BOB heating. They are affected much less by a weak in situ heating in 2 or 3 days. Nevertheless, the model-induced heating and circulation at day 7 in the CH2 run (Fig. 9i) are quite similar to the observed patterns on 17 or 19 May (Figs. 3g and 3i). This result suggests that the appearance of westerlies as well as convection (and the associated condensation heating) over the NSCS that occurs just before the SCSSM onset could at least be partly a Rossby wave type of atmospheric response to the intensified convective heating over the BOB.

The locations of the $u = 0$ isotachs at day 1 (Fig. 9b) differ very little from the initial field. Compared with those observed in the middle of May (Fig. 3b), the model simulation shows a very strong vertical wind shear. This suggests that the use of the global zonal mean as the initial fields possesses a strong winter-type meridional temperature gradient. From day 5, the tilting of the ridge surface over the SCS domain has been reduced (Fig. 9f). On day 7, the locations of this isotach at 200 and 500 hPa are very close due to the condensation

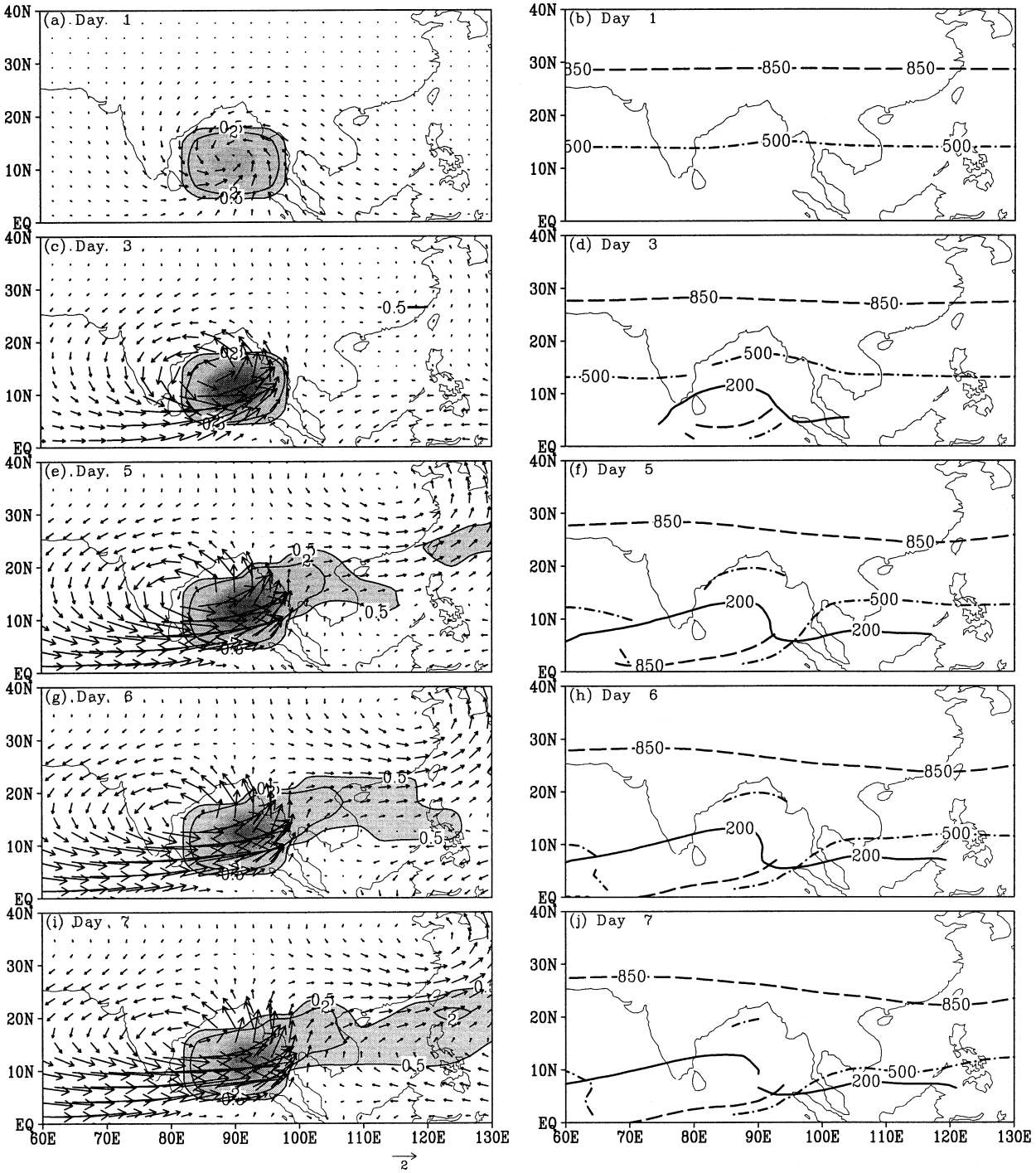

FIG. 9. (left) Condensation heating (shaded, contour interval: 0.5, 2, 4, 6, 8, 10 . . . K d^{-1}) and perturbation wind vector at 850 hPa (m s^{-1}); and (right) zero isotachs of the zonal wind u where the meridional gradient of u is positive at 200, 500, and 850 hPa in the CH2 run. The days from the initial time are labeled on each panel.

heating over the NSCS (Fig. 9j). However, the tilting pattern is still the winter type. This is partly because the initial meridional temperature gradient is too large to be reversed, and partly because the model-induced heating over the NSCS is too weak (no deep convective parameterization process is included in the experiment). Despite this discrepancy, the results shown in the right-hand side of Fig. 9 indicate that the condensation heating over the NSCS generated by the BOB monsoon forcing does contribute to the in situ warming, and contribute

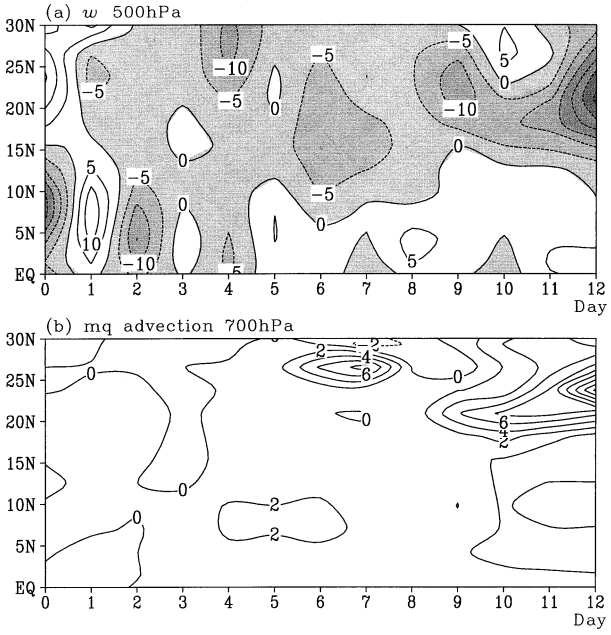

FIG. 10. Time–latitude cross section from day 0 (initial field) to day 12 in the CH2 run of (a) vertical *p*-velocity at 500 hPa (10^{-3} Pa s^{-1}) and (b) the horizontal advection of moisture mass *mq* at 700 hPa (10^{-9} kg m^{-2} s^{-1}) averaged over 110°–120°E.

to the weakening of the wintertime meridional gradient of temperature over the SCS region.

d. No BOB monsoon heating experiment

Although the two sensitivity experiments have provided new insights to the two problems raised in the introduction, they do not result in the SCSSM onset. A simple consideration suggests that the time (Δt) needed to overturn the initial wintertime meridional gradient of temperature [$(\partial T/\partial y)_0 < 0$] depends upon the meridional gradient of the heating rate ($\partial Q/\partial y$) averaged before the monsoon onset, that is,

$$\Delta t = -\frac{(\partial T/\partial y)_0}{(\partial Q/\partial y)}. \tag{5}$$

The heating rate Q represents both internal and external forcing. For a certain meridional gradient of heating rate, the time needed for the monsoon onset then depends upon the initial meridional gradient of temperature. Therefore it becomes clear that the too-strong wintertime meridional gradient of temperature imposed in experiments CH1 and CH2 cannot be overturned within a short period by the heating gradient.

To overcome this, an experiment with more realistic initial fields needs to be carried out. In this experiment (NOCH—no condensation heating), the model integration is the same as the control (CON) run except that the convective and large-scale condensation heating over the BOB and Indochina region (2°–26°N, 80°–112°E) are removed from the thermodynamic equation. Such an area is larger than the BOB. This is because the heating over the Indochina peninsula is the side effect of the BOB forcing, as is evident from Figs. 6 and 9e (day 5 of the integration). The differences between the CON and NOCH runs may then reveal to some extent the atmospheric responses to the BOB heating. The NOCH experiment starts from 12 May of the CON run. This date is chosen because it is within the BOB monsoon onset in the CON run.

On day 1, the response is localized (Fig. 11a). From day 4 to day 7, westerly winds and condensation heating over the Indochina peninsula and northern SCS are observed, which mimics the asymmetric Rossby wave response (Figs. 11b,c). Such responses became much stronger at day 11, and expanded southeastward (Fig. 11d). The 850-hPa wind field difference between the two experiments shows a trough over the SCS domain, and the subtropical anticyclone has retreated eastward to the western Pacific (Fig. 11d). In other words, condensation heating over the BOB and Indochina is responsible for weakening (strengthening) the anticyclonic circulation over the SCS (western Pacific). As a result, by day 11 in the CON run, westerly winds and deep convection dominated most of the SCS domain (Fig. 11e) and hence the onset of the SCSSM.

To understand this further, it is noted that in the CON run, the locations of the ridge of the subtropical anticyclone at 500 hPa is to the south of that at 850 hPa at day 1 and no easterlies are found at 200 hPa (Fig. 12a), which suggests that the circulation is still in a winter pattern. Ten days later, after the condensation heating has warmed up the NSCS, the temperature field changes significantly. Except at the middle level (500 hPa), the temperature has increased largely over the northern SCS (Fig. 12b). In the upper troposphere between 500 and 200 hPa, the warming over the NSCS is >1.5°C, much stronger than that over the southern SCS. As a result, the tilting of the ridge surface over the SCS domain changes from the winter pattern at day 1 (Fig. 12a) to the summer pattern at day 11 (Fig. 12c). This means the anticyclone at 850 hPa has moved southward and retreated from the SCS region (Fig. 11e), and the onset of a SCS monsoon occurs. All the results obtained from these sensitivity experiments lead us to the following conclusion: it is this horizontal differential heating across the SCS domain that contributes to the overturning of the horizontal temperature gradients, and the SCS monsoon onset.

4. Summary discussion and concluding remarks

The onset of the Asian summer monsoon (ASM) marks the transition from winter to summer of the circulation over the tropical and subtropical areas of Asia. Our understanding of its onset processes has progressed gradually in the twentieth century. Since the late 1980s, after the study of Tao and Chen (1987), it has been widely agreed that the earliest onset of the Asian mon-

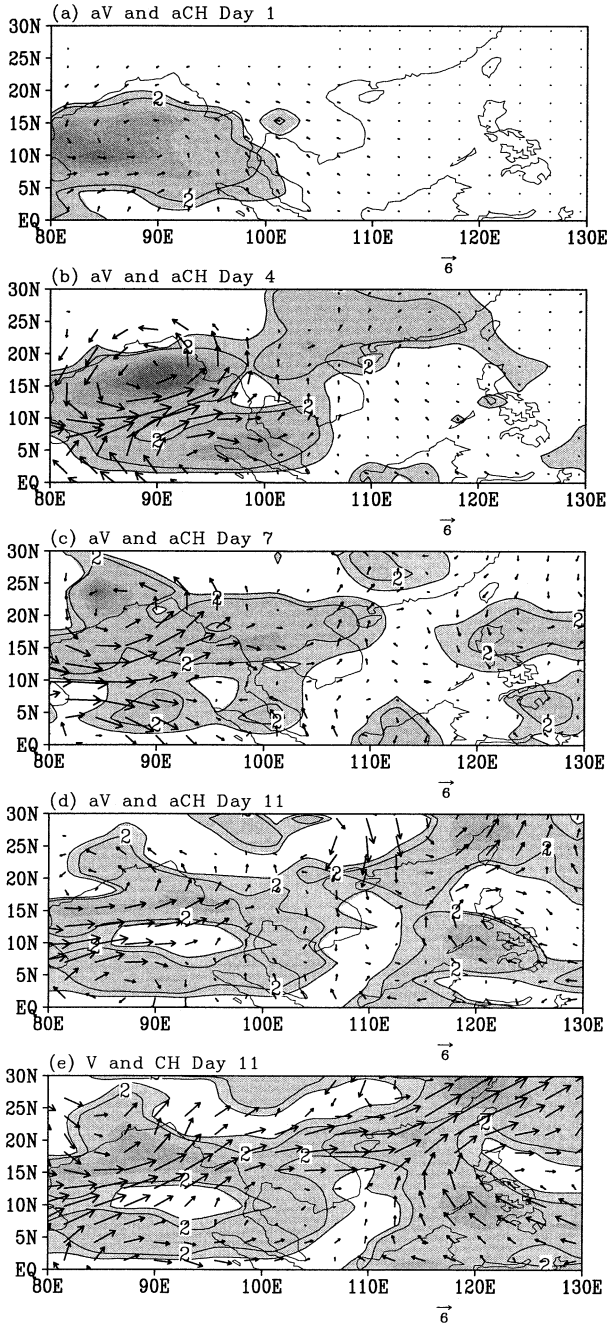

FIG. 11. Difference between the CON and NOCH (CON-NOCH) runs of condensation heating at 400 hPa (shaded, interval: 0.5, 2, 4, 6, 8, 10 . . . K d^{-1}) and wind vectors at 850 hPa (m s^{-1}) at (a) day 1, (b) day 4, (c) day 7, and (d) day 11. (e) Condensation heating at 400 hPa (shaded) and wind vectors at 850 hPa (m s^{-1}) at day 11 in the CON run.

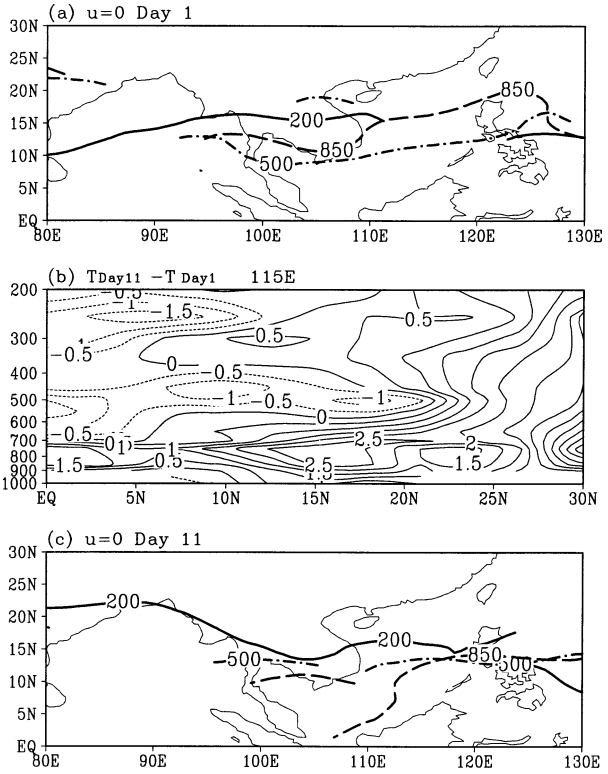

FIG. 12. The ridge axis (zero isotach of zonal wind *u* and meridional gradient of *u* positive) at 200, 500, and 850 hPa at (a) day 1 (13 May) and (c) day 11. (b) Vertical–latitude cross section of temperature difference between day 11 and day 1 along 115°E derived from the CON run.

soon occurs over the South China Sea (SCS) in mid-May, and then the onset propagates westward continuously to reach the south Asia subcontinent by early June. With the availability of other datasets [such as the National Center for Atmospheric Research–National Centers for Environmental Prediction (NCAR–NCEP) reanalysis] in the 1990s, many new insights have been proposed. It was found that the onset of the ASM occurs in three distinct consecutive stages in most cases: first over the Bay of Bengal (BOB), then over the SCS, and last over the Indian subcontinent (Wu and Zhang 1998; Wu and Chan 2000; Xu and Chan 2001; Fong and Wang 2001). One of the significant changes in circulation during the monsoon onset is in the configuration of the subtropical anticyclone. Its ridge surface tilts southward with increasing height before the onset, but northward after the onset (Mao et al. 2002), and the onsets over the BOB and the SCS are accompanied by the development of a depression and an eastward retreat of the subtropical anticyclone in the lower troposphere (Lau et al. 2000; Xu and Chan 2001). In addition to confirming these conclusions using the data from the 1998 case, this study attempts to understand the underlying mechanisms, particularly the link between the SCS monsoon onset and the deep convection of the monsoon vortex over the BOB through numerical simulations.

Soon after the BOB monsoon onset, the ridge surface tilts northward over the BOB, but southward over the SCS. As a result, in the lower troposphere, cyclonic flow dominates the BOB region while the SCS is still controlled by the subtropical anticyclone, and deep convection develops over the BOB and Indochina area. The

condensation heating associated with this heating has significant impacts on the atmospheric circulation:

- The in situ southerlies at low levels become stronger, resulting in the intensification of the cyclone to the west and anticyclone to the east. Such intensified southerlies and southwesterlies advect much water vapor to the north of the enhanced anticyclone, and cause the development of westerlies and an increase in low-level moisture along the coast of south China, which was also observed by Chan et al. (2000).
- The deep condensation heating over the BOB generates an asymmetric Rossby wave, which is characterized by ascent to its east and descent to its west. Along the coast of south China, such ascent occurs in coordination with the moistened air, which likely helps the release of the convective available potential energy (CAPE), as suggested by Chan et al. (2000).
- The deep convective heating over the BOB also generates a Rossby wave train with its anticyclone phase located over the northern part of the Indochina peninsula and southwest China, and its second cyclonic phase over east China. The westerlies to the south of the second cyclone thus enhance those north of the subtropical anticyclone over the SCS. The northerly and northwesterly flow to the east of the forced anticyclone, on the other hand, brings cold air from the subtropics to the moistened area along the south China coast, which then contributes to the release of CAPE as well.

In their study of the SCS monsoon onset, Chang and Chen (1995) found that the midlatitude front north of the SCS region was the trigger for the onset. Chan et al. (2000) investigates the onset case of 1998, and also found that a cold front passage through the northern part of the SCS before the SCS monsoon onset helped the release of CAPE, which then led to the onset. The results revealed in this study show a Rossby wave train emanates from the heating region and propagates northeastward (Figs. 8 and 9). The cold air invasion to the SCS region itself is at least partly a lower-tropospheric response to the deep convective heating over the BOB in association with such a Rossby wave train. This conclusion is supported by the two sensitivity numerical experiments in this study. In these experiments, although the initial flows are zonal symmetric, the imposed deep convective heating over the BOB does produce a band of westerlies and condensation heating along the coast of south China, and brings northerlies from higher latitudes (see Figs. 8 and 9).

The significance of the formation of the high CAPE band over the northern SCS (NSCS) and the release of this CAPE is also investigated in this study. It is shown that the deep condensation heating in the upper troposphere due to this release of CAPE warms the air column over the NSCS, overturning the meridional temperature gradient, and hence the tilting of the ridge surface over the SCS from the winter to the summer type. As a result, the low-level subtropical anticyclone that occupies the SCS is replaced by a cyclonic circulation and anticyclone circulation that is restricted to the western Pacific. Westerlies and southerlies dominate the entire SCS domain; deep convection also develops, and the monsoon onset over SCS occurs. All of these results lead to the following conclusion: it is the development of deep convection over the Bay of Bengal after the BOB monsoon onset that creates favorable conditions for the monsoon onset over South China Sea to occur. Although this is a case study, the results are generally applicable since in most years the BOB convection precedes the SCS monsoon onset.

Prediction of the ASM onset is an important but complicated issue in short-term climate forecasting. A careful diagnosis of the analysis date reveals that the monsoon onset over the BOB always occurs prior to monsoon onset over the SCS by a certain period, which can vary from a few days to more than one month (Wu and Chan 2000; Mao et al. 2002). If the meridional temperature gradient across the ridge surface over the SCS after the BOB monsoon onset is known, and the gradient of diabatic heating can be estimated, then the date of monsoon onset over the SCS might be predicted using Eq. (5). In any case, a better prediction depends on a better understanding of the processes involved. To achieve this goal, many more efforts in understanding the physical processes of the Asian monsoon onset are required.

Acknowledgments. The authors would like to thank the Beijing Data Center of SCSMEX for providing the gridded regional assimilated analysis data. Reynolds SST data are provided by the NOAA–CIRES Climate Diagnostics Center, Boulder, Colorado, from their Web site at http://www.cdc.noaa.gov/. Interpolated NCAR OLR are provided by the NOAA Climate Diagnostics Center. The authors would like to thank Dr. Paquita Zuidema of NOAA/Environmental Technology Laboratory and another anonymous reviewer for many constructive comments on an earlier version of the manuscript.

Much of the work of the first author was carried out during her visit to the City University of Hong Kong supported through the Croucher Foundation Visitorship Scheme. This research was also partly supported by the Natural Science Foundation of China under Grant 49905002 and 40135020, and by the Chinese Academy of Sciences Grant ''Hundred Talents'' for ''Validation of Coupled Climate Models.'' Publication of this paper was supported by City University of Hong Kong Grant 7010010.

REFERENCES

Boville, B. A., and P. R. Gent, 1998: The NCAR climate system model, version one. *J. Climate,* **11,** 1115–1130.

Chan, J. C. L., Y. G. Wang, and J. J. Xu, 2000: Dynamic and thermodynamic characteristics associated with the onset of the 1998 South China Sea summer monsoon. *J. Meteor. Soc. Japan,* **78,** 367–380.

Chang, C. P., and G. T. J. Chen, 1995: Tropical circulation associated with southwest monsoon onset and westerly surges over the South China Sea. *Mon. Wea. Rev.,* **123,** 3254–3267.

Chen, P., M. P. Hoerling, and R. M. Dole, 2001: The origin of the subtropical anticyclones. *J. Atmos. Sci.,* **58,** 1827–1835.

Ding, Y. H., and C. Y. Li, Eds., 1999: *Onset and Evolution of the South China Sea Monsoon and Its Interaction with the Ocean.* Chinese Meteorological Press, 422 pp.

——, and Y. Liu, 2001: Onset and the evolution of the summer monsoon over the South China Sea during SCSMEX Field Experiment in 1998. *J. Meteor. Soc. Japan,* **79,** 255–276.

Ertel, H., 1942: Ein neuer hydrodynamische wirbdsatz. *Meteor. Z. Braunschweig,* **59,** 277–281.

Fong, S. K., and A. Y. Wang, 2001: *Climatological Atlas for Asian Summer Monsoon.* Macau Foundation, 318 pp.

Gill, A. E., 1980: Some simple solutions for heat-induced tropical circulation. *Quart. J. Roy. Meteor. Soc.,* **106,** 447–662.

Hack, J. J., 1994: Parameterization of moist convection in the National Center for Atmospheric Research Community Climate Model (CCM2). *J. Geophys. Res.,* **99,** 5551–5568.

Hoskins, B. J., 1996: On the existence and strength of the summer subtropical anticyclones. *Bull. Amer. Meteor. Soc.,* **77,** 1287–1292.

Kiehl, J. T., J. J. Hack, G. B. Bonan, B. A. Boville, B. P. Briegleb, D. L. Williamson, and P. J. Rasch, 1996: Description of the NCAR Community Climate Model (CCM3). NCAR Tech. Note NCAR/TN-420+STR, 152 pp. [Available from NCAR, P.O. Box 3000, Boulder, CO 80307.]

Krishnamurti, T. N., P. Ardanuy, Y. Ramanathan, and R. Pasch, 1981: On the onset vortex of the summer monsoon. *Mon. Wea. Rev.,* **109,** 344–363.

Lau, K. M., H. T. Wu, and S. Yang, 1998: Hydrologic processes associated with the first transition of the Asian summer monsoon: A pilot satellite study. *Bull. Amer. Meteor. Soc.,* **79,** 1871–1882.

——, and Coauthors, 2000: A report of the field operations and early results of the South China Sea Monsoon Experiment (SCSMEX). *Bull. Amer. Meteor. Soc.,* **81,** 1261–1270.

Li, C. Y., and X. Qu, 1999: Characteristics of atmospheric circulation associated with summer monsoon onset in the South China Sea. *Onset and Evolution of the South China Sea Monsoon and Its Interaction with the Ocean,* Y. Ding and C. Li, Eds., China Meteorological Press, 200–209.

Lin, P.-H., M.-D. Chou, S.-C. Tsay, and G. R. Liu, 1998: Surface radiation budget analysis at Dongsha during SCSMEX. *Proc. IX Pacific Science Inter-Congress, Asian Pacific Monsoon and Typhoon Meteorology Symp.,* Taipei, Taiwan, 87–89. [Available from linpo@atmos.as.ntu.edu.tw.]

Liu, Y. M., G. X. Wu, H. Liu, and P. Liu, 2001a: Condensation heating of the Asian summer monsoon and the subtropical anticyclone in the Eastern Hemisphere. *Climate Dyn.,* **17,** 327–338.

——, ——, R. C. Yu, and X. Liu, 2001b: Thermal adaptation, overshooting, dispersion, and subtropical anticyclone. II: Horizontal inhomogeneous heating and energy dispersion. *China J. Atmos. Sci.,* **25,** 317–328. [Available in Chinese with English abstract from lym@lasg.iap.ac.cn.]

Mao, J. Y., G. X. Wu, Y. Liu, P. Liu, and W. Li, 2002: Study on modal variation of subtropical high and its mechanism during seasonal transition. Part I: Climatological features of subtropical high structure. *Acta Meteor. Sin.,* **60,** 1–9. [Available in Chinese with English abstract from lym@lasg.iap.ac.cn.]

Reynolds, R. W., and T. M. Smith, 1994: Improved global sea surface temperature analyses using optimum interpolation. *J. Climate,* **7,** 929–948.

Rodwell, M. R., and B. J. Hoskins, 1996: Monsoons and the dynamics of deserts. *Quart. J. Roy. Meteor. Soc.,* **122,** 1385–1404.

——, and ——, 2001: Subtropical anticyclones and summer monsoons. *J. Climate,* **14,** 3192–3211.

Tao, S. Y., and L. X. Chen, 1987: A review of recent research on the East Asia summer monsoon in China. *Monsoon Meteorology,* C. P. Chang and T. N. Krishnamurti, Eds., Oxford University Press, 60–92.

Wu, G. X., and Y. S. Zhang, 1998: Tibetan Plateau forcing and the timing of the monsoon onset over south Asia and the South China Sea. *Mon. Wea. Rev.,* **126,** 913–927.

——, Y. M. Liu, and P. Liu, 1999: The effect of spatially non-uniform heating on the formation and variation of subtropical high. Part I: Scale analysis. *Acta Meteor. Sin.,* **57,** 257–263. [Available in Chinese with English abstract from lym@lasg.iap.ac.cn.]

Wu, K. W., and J. C. L. Chan, 2000: Intraseasonal and interannual variabilities of the South China Sea summer monsoon. *Proc. Int. Conf. on Climate and Environment Variability and Predictability,* Shanghai, China, 69. [Available from lym@lasg.iap.ac.cn.]

Xu, J., and J. C. L. Chan, 2001: First transition of the Asian summer monsoon in 1998 and the effect of the Tibet–Tropical ocean thermal contrast. *J. Meteor. Soc. Japan,* **79,** 241–253.

Zhang, G. J., and N. A. McFarlane, 1995: Sensitivity of climate simulations to the parameterization of cumulus convection in the Canadian Climate Centre General Circulation Model. *Atmos.–Ocean,* **33,** 407–446.

Zhang, Y. S., and G. X. Wu, 1998: Diagnostic investigations of mechanism of onset of Asian summer monsoon and abrupt seasonal transitions over Northern Hemisphere, Part I. *Acta Meteor. Sin.,* **56,** 513–527. [Available in Chinese with English abstract from lym@lasg.iap.ac.cn.]